AMERICAN SOCIETY FOR MICROBIOLOGY | Antimicrobial Agents and Chemotherapy®

PHARMACOLOGY

# Pharmacokinetics of Pyrazinamide and Optimal Dosing Regimens for Drug-Sensitive and -Resistant Tuberculosis

**Maxwell T. Chirehwa,[a] Helen McIlleron,[a] Roxana Rustomjee,[b]* Thuli Mthiyane,[c]* Philip Onyebujoh,[d] Peter Smith,[a] Paolo Denti[a]**

Division of Clinical Pharmacology, Department of Medicine, University of Cape Town, Cape Town, South Africa[a]; Strategic Health Innovation Partnerships (SHIP), South African Medical Research Council, Cape Town, South Africa[b]; TB Research Unit, Clinical and Biomedical, South African Medical Research Council, Durban, South Africa[c]; Intercountry Support Team for East and Southern Africa, World Health Organization, Regional Office for Africa, Harare, Zimbabwe[d]

**ABSTRACT** Pyrazinamide is used in the treatment of tuberculosis (TB) because its sterilizing effect against tubercle bacilli allows the shortening of treatment. It is part of standard treatment for drug-susceptible and drug-resistant TB, and it is being considered as a companion drug in novel regimens. The aim of this analysis was to characterize factors contributing to the variability in exposure and to evaluate drug exposures using alternative doses, thus providing evidence to support revised dosing recommendations for drug-susceptible and multidrug-resistant tuberculosis (MDR-TB). Pyrazinamide pharmacokinetic (PK) data from 61 HIV/TB-coinfected patients in South Africa were used in the analysis. The patients were administered weight-adjusted doses of pyrazinamide, rifampin, isoniazid, and ethambutol in fixed-dose combination tablets according to WHO guidelines and underwent intensive PK sampling on days 1, 8, 15, and 29. The data were interpreted using nonlinear mixed-effects modeling. PK profiles were best described using a one-compartment model with first-order elimination. Allometric scaling was applied to disposition parameters using fat-free mass. Clearance increased by 14% from the 1st day to the 29th day of treatment. More than 50% of patients with weight less than 55 kg achieved lower pyrazinamide exposures at steady state than the targeted area under the concentration-time curve from 0 to 24 h of 363 mg · h/liter. Among patients with drug-susceptible TB, adding 400 mg to the dose for those weighing 30 to 54 kg improved exposure. Average pyrazinamide exposure in different weight bands among patients with MDR-TB could be matched by administering 1,500 mg, 1,750 mg, and 2,000 mg to patients in the 33- to 50-kg, 51- to 70-kg, and greater than 70-kg weight bands, respectively.

**KEYWORDS** NONMEM, population pharmacokinetics, HIV/TB coinfection, fat-free mass, AUC, weight band dosing

**Received** 7 March 2017 **Returned for modification** 31 March 2017 **Accepted** 24 May 2017

**Accepted manuscript posted online** 12 June 2017

**Citation** Chirehwa MT, McIlleron H, Rustomjee R, Mthiyane T, Onyebujoh P, Smith P, Denti P. 2017. Pharmacokinetics of pyrazinamide and optimal dosing regimens for drug-sensitive and -resistant tuberculosis. Antimicrob Agents Chemother 61:e00490-17. https://doi.org/10.1128/AAC.00490-17.



Address correspondence to Paolo Denti, paolo.denti@uct.ac.za.

* Present address: Roxana Rustomjee, Tuberculosis Clinical Research Branch, Therapeutics Research Program, Division of AIDS/NIAID/NIH/DHHS, Rockville, MD, USA; Thuli Mthiyane, TB Platform, Medical Research Council, Pretoria, South Africa.

Pyrazinamide is a prodrug converted to its active form, pyrazinoic acid, by hepatic microsomal deamidase (1) and is active against dormant and semidormant *Mycobacterium tuberculosis* bacilli, especially in acidic environments (2, 3). It is currently part of a four-drug fixed-dose combination (FDC), which includes isoniazid, ethambutol, and rifampin, an inducer of a number of cytochrome P450 enzymes via the pregnane X receptor (PXR) (4). Pyrazinamide is currently being considered as a companion drug in novel tuberculosis (TB) treatment regimens (5–7), including for multidrug-resistant tuberculosis (MDR-TB).

Interest in the drug derives from its potent sterilizing activity, which confers the ability to shorten treatment duration. Pyrazinamide exposures have been correlated with favorable treatment outcomes in patients on standard doses (5, 8–13). A pyrazi-

**TABLE 1** Baseline characteristics of patients

| Characteristic or parameter | Value[a] |
|---|---|
| Total no. | 61 |
| Females, *n* (%) | 33 (54) |
| Receiving ART, *n* (%) | 41 (67) |
| Treatment 5 days/week, *n* (%) | 51 (84) |
| Age (yr) | 32 (18–47) |
| Weight (kg) | 55.2 (34.4–98.7) |
| Height (m) | 1.59 (1.41–1.81) |
| FFM (kg) | 42.2 (28.0–57.6) |
| Albumin (g/liter) | 26 (15–43) |
| ALT (U/liter) | 16 (5–44) |
| Creatinine ($\mu$mol/liter) | 74 (53–155) |
| Viral load ($\times$1,000) (copies/ml) | 86 (0.05–13,000) |
| $CD4^+$ count (cells/liter) | 254 (12–500) |

[a]Values are expressed as median (range) unless otherwise specified.

namide area under the concentration-time curve from 0 to 24 h ($AUC_{0-24}$) of at least 363 mg · h/liter has been associated with long-term TB treatment outcomes among patients with drug-susceptible TB and could be targeted for treatment optimization (5). The current recommended weight-adjusted daily dose of pyrazinamide for treatment of drug-susceptible TB is approximately 25 (range, 20 to 30) mg/kg of body weight (14), while that for treatment of MDR-TB is about 35 (range, 30 to 40) mg/kg (15). Doses higher than those currently recommended may result in high levels of 5-hydroxypyrazinoic acid, which is responsible for pyrazinamide induced hepatotoxicity (16). On the other hand, there exist discrepancies in exposure between the weight bands; patients in the lower weight bands achieve lower drug exposures (17, 18).

Despite interest in pyrazinamide, relatively few studies have described its pharmacokinetics (PK) longitudinally (19–22). We previously reported PK exposures of pyrazinamide in this cohort of HIV/TB-coinfected patients (17). Here, we use a population modeling approach to describe changes in PK parameters during the first month of treatment and identify other factors affecting the PK. We then used parameter estimates of the final model to simulate exposures associated with a range of feasible doses for treatment of drug-susceptible TB and MDR-TB.

## RESULTS

**Demographic characteristics.** Pyrazinamide concentration data for 61 HIV/TB-coinfected patients were available for analysis. Demographic characteristics of these patients have been reported previously (17), and a summary is provided in Table 1. A total of 1,342 plasma samples were included in the analysis. One sample had a concentration below the lower limit of quantification and was discarded.

**Structural model and parameter estimates.** Pyrazinamide pharmacokinetics was best described by a one-compartmental model with first-order elimination and transit compartment absorption. Table 2 shows the parameter estimates of the final model and their 95% bootstrap confidence interval. Clearance (CL) was found to increase by 14% on day 29 from a typical value of 3.35 liters/h on day 1; thus, day 29 clearance would be estimated at 3.83 liters/h (change in objective function value [ΔOFV] of $-21$ compared to a model with one estimate for clearance, 1 degree of freedom [df], and a *P* value of $<0.001$). This process was best described using a linear model, which was more parsimonious than estimating separate values of CL. The clearance estimates for day 1 and day 29 obtained using a linear model were similar to the ones obtained by estimating separate clearance values on the 4 days. The latter model estimated clearance values of 3.35 liters/h on day 1, 3.46 liters/h on day 8, 3.66 liters/h on day 15, and 3.82 liters/h on day 29. Using the arguably more biologically plausible exponential model did not significantly improve the fit and could not provide a robust estimate of the half-life of the induction, sometimes producing implausible results in the bootstrap analysis. The absorption process was best characterized using the transit compartment absorption, which provided significant improvement compared to simple first-order

**TABLE 2** Estimated parameter values from the final model

| Parameter | Estimate | Bootstrap 95% CI[a] | Shrinkage (%) |
|---|---|---|---|
| $CL/F_{day\ 1}$[b] (liter/h) | 3.35 | 3.11–3.56 | |
| $\Delta CL/F_{day\ 29}$ (%) | 14.3 | 6.0–25.8 | |
| $V/F$[b] (liter) | 43.2 | 41.5–44.7 | |
| $k_a$[e] ($h^{-1}$) | 3.54 | 3.0–4.27 | |
| MTT[f] (h) | 0.542 | 0.47–0.61 | |
| NN[c] | 28 | 7–52 | |
| $F$[d] | 1 fixed | | |
| Between-subject variability (%) | | | |
| CL | 16.3 | 11.0–20.0 | 12.8 |
| $F$ | 10.7 | 7.6–13.2 | 18.5 |
| Between-occasion variability (%) | | | |
| CL | 13.3 | 10.0–15.4 | 31.5 |
| $F$ | 11.9 | 8.5–15.5 | 13.5 |
| $k_a$ | 84.0 | 79.7–97.5 | 30.3 |
| MTT | 52.9 | 40.1–68.7 | 39.9 |
| Error | | | |
| Additive (mg/liter) | 1.23 | 0.85–1.57 | |
| Coefficient of variation (%) | 4.4 | 2.8–5.4 | |

[a]CI, confidence interval.
[b]This parameter has been adjusted by allometric scaling, and the values reported refer to a subject with FFM of 42 kg (the median value of the cohort). The individual estimates for clearance and volume parameters were defined as $CL_i = \theta_{CL}(FFM_i/42)^{0.75} \cdot e^{(BSVCL\ +\ BOVCL)}$ and $V_i = \theta_v(FFM_i/42)^1$, respectively. $\theta_{CL}$ is the typical values for clearance and $\theta_v$ is the typical value for volume of distribution.
[c]NN, number of absorption transit compartments.
[d]$F$, bioavailability.
[e]$k_a$, absorption rate constant.
[f]MTT, mean transit time.

absorption with a delay using a lag (ΔOFV of −37, 1 df, $P$ value of <0.001). On average, the time from drug ingestion to absorption is around half an hour and then is followed by very fast absorption. Large variability (>50%) in absorption between occasions was observed. The model also identified between-subject variability in clearance and bioavailability as well as between-occasion variability in clearance, bioavailability, and absorption mean transit time.

Inclusion of allometric scaling on CL and volume of distribution ($V$) using total body weight (TBW) improved the fit (ΔOFV of −13), but the better predictor to adjust PK for body size was fat-free mass (FFM), which dramatically reduced the OFV further when changed to TBW (ΔOFV of −37). Estimating allometry exponents did not result in a significant improvement in OFV and the estimated values were close, 0.75 for CL and 1 for $V$, hence the exponents were fixed to these literature values. After the inclusion of allometric scaling, the model could not detect any additional effect of $CD4^+$ count, viral load, early antiretroviral therapy (ART) initiation, alanine transaminase (ALT), albumin, creatinine clearance, and formulation. The visual predictive check plot in Fig. 1 shows that our model correctly describes the observed concentrations and captures the change in clearance over time.

**Monte Carlo simulations.** The median weight, height, and FFM of the 870 patients with drug-susceptible TB were 53 kg (range, 30 to 102 kg), 1.65 m (range, 1.35 to 1.98 m), and 40.7 kg (range, 25.3 to 71.7 kg), respectively, with 45% being female. Figure 2 shows the simulated exposures at day 29 of treatment achieved under dosing strategies for the treatment of drug-susceptible TB. With the currently recommended weight-adjusted dose, patients in the lower weight bands are exposed to much lower levels of pyrazinamide, with patients of <38 kg being exposed to 42% lower $AUC_{0-24}$ than those weighing >70 kg. The proportion of patients achieving a target $AUC_{0-24}$ of 363 mg · h/liter in each weight band is presented in Table 3. The model predicts that at the current dose, only around 10% of the patients in the 30- to 37-kg weight band and 40% in the 38- to 55-kg weight band achieve the target exposure. Alternative dosing

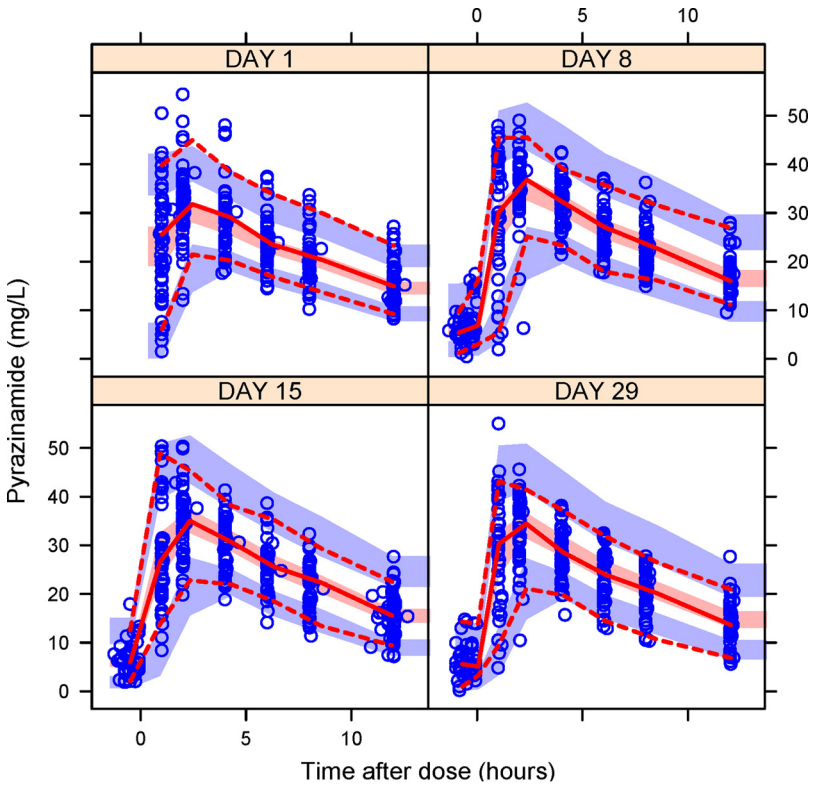


**FIG 1** Visual predictive check. Open circles are the observed concentrations. The middle continuous line is the 50th percentile of the observed data, and upper and lower dashed lines are the 97.5th and 2.5th percentiles of the observed data, respectively. The shaded regions represent the 95th prediction interval of the 2.5th, 50th, and 97.5th percentiles.

approaches minimizing the difference in exposure between weight bands without changing the weight bands are depicted in Fig. 2. In the most balanced alternative, alternative 2 (administering 1,200 mg to patients in the 30- to 37-kg weight band and 1,600 mg to those in the 38- to 54-kg weight band; other patients' dosing remained unchanged), the highest median exposure would be in the >70-kg weight band while the lowest will be in the 55- to 70-kg weight band, resulting in a maximum difference in exposure of 16%. The simulations show that overall, 73% of the patients will achieve target exposure with alternative 2 dosing strategies compared to 51.5% for the current dosing strategy. Figure 3a and b show simulated concentrations for two typical male patients of weights of 34 kg and 46 kg achieved with the current dose and alternative dosing strategy 2. The two typical patients attain a maximum concentration of drug in serum ($C_{max}$) of at least 35 mg/liter when dosing is administered per alternative strategy 2. As shown in Fig. 2, alternative dosing strategies 1 and 3 do not seem to minimize differences in exposure between weight bands, and some patients in the lower weight bands would achieve extremely high exposure when dosed using the alternative strategy 3.

Figure 4 shows simulated steady-state pyrazinamide $AUC_{0-24}$ achieved with doses within the recommended range of 1,000 mg to 2,500 mg for the treatment of MDR-TB. Simulations were performed using estimated PK parameters for day 1 without the increase in clearance, which may be due to coadministration with rifampin. Pyrazinamide exposure associated with the currently recommended dose is only comparable if patients in the 33- to 50-kg weight band are administered 1,500 mg, while patients in the 51- to 70-kg and >70-kg bands receive 1,750-mg and 2,000-mg doses, respectively. These doses ensure that on average, at least 90% of patients in the three weight bands achieve an $AUC_{0-24}$ of at least 363 mg · h/liter. On the other hand, administering

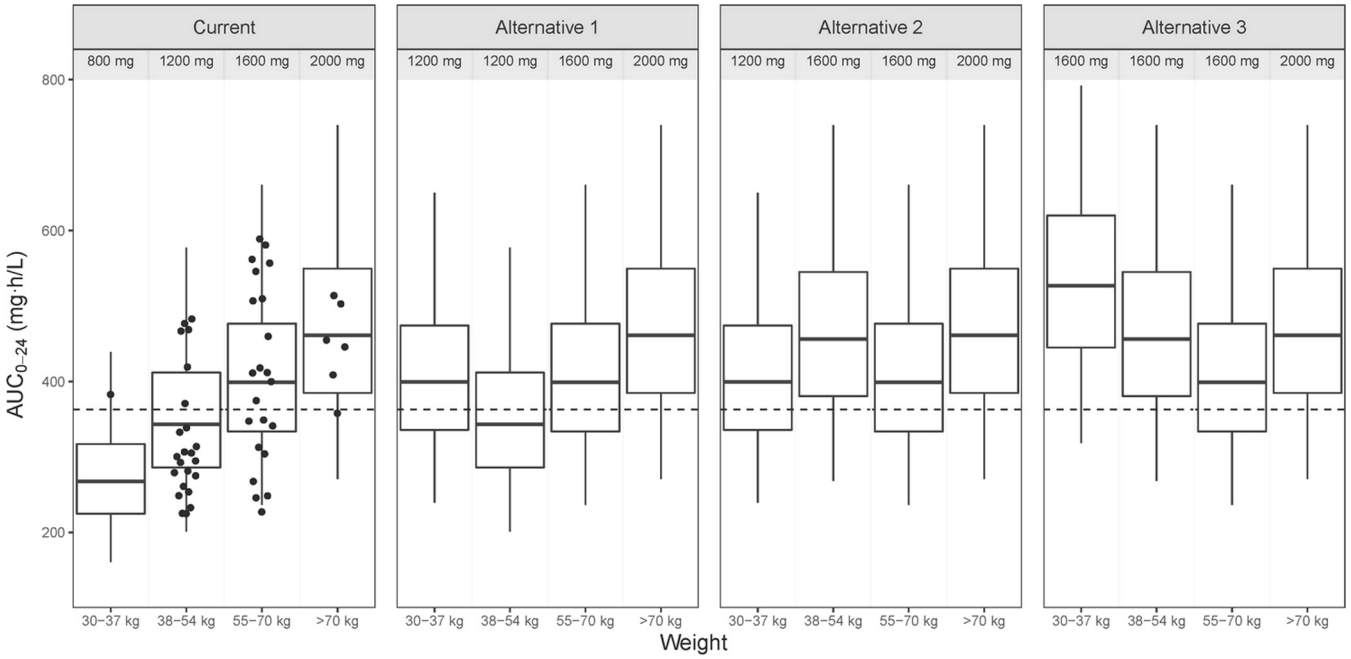


**FIG 2** Box plots of simulated $AUC_{0-24}$ for currently recommended doses for drug-susceptible TB (14) and 3 alternative dosing strategies, stratified by weight band. Dots are the observed $AUC_{0-24}$ on day 29 of treatment. The dashed line represents an $AUC_{0-24}$ of 363 mg · h/liter. The dosing strategies used for the 30- to 37-, 38- to 54-, 55- to 70-, and >70-kg weight bands are 800 mg, 1,200 mg, 1,600 mg, and 2,000 mg for current doses. For alternative dosing strategy 1, patients weighing 30 to 37 kg receive 1,200 mg, while the doses for patients in the other weight bands are unchanged. For alternative 2, 1,200-mg and 1,600-mg doses are administered to patients weighing 30 to 37 kg and 38 to 54 kg, respectively, while other patients' dosing is unchanged. For alternative 3 dosing, 1,600 mg is administered to patients weighing 30 to 54 kg and dosing for other patients is unchanged.

1,000 mg or 1,200 mg to patients in the 33- to 50-kg weight band results in only 41% and 68% of them attaining an $AUC_{0-24}$ of 363 mg · h/liter.

## DISCUSSION

We described the population pharmacokinetics of pyrazinamide among HIV/TB-coinfected patients during the first month of treatment using nonlinear mixed-effects modeling. The model described an increase in pyrazinamide clearance with days on treatment (from day 1 to day 29) and identified FFM as the best predictor of the effect of body size on exposure compared to total body weight. Simulations were used to explore pyrazinamide exposure achieved with different dosing strategies for the treatment of drug-susceptible and multidrug-resistant TB.

FFM is calculated based on weight, height, and sex and was found to be superior to total body weight when included in the model via allometric scaling to capture the effect of body size on differences in CL/*F* and *V*/*F* (23). Some previously proposed population PK models of pyrazinamide do not account for the effect of body size using allometric scaling (19, 21). One of these, by Wilkins et al. (19), described a linear effect

**TABLE 3** Proportion of simulated patients with drug-susceptible TB achieving a target $AUC_{0-24}$ of 363 mg · h/liter

| Dose (mg) | Weight (kg) | Proportion (%) |
|---|---|---|
| 800 | 30–37 | 11.4 |
| 1,200 | 30–37 | 64.6 |
| | 38–54 | 41.9 |
| 1,600 | 30–37 | 93.4 |
| | 38–54 | 80.4 |
| | 55–70 | 64.1 |
| 2,000 | >70 | 81.5 |

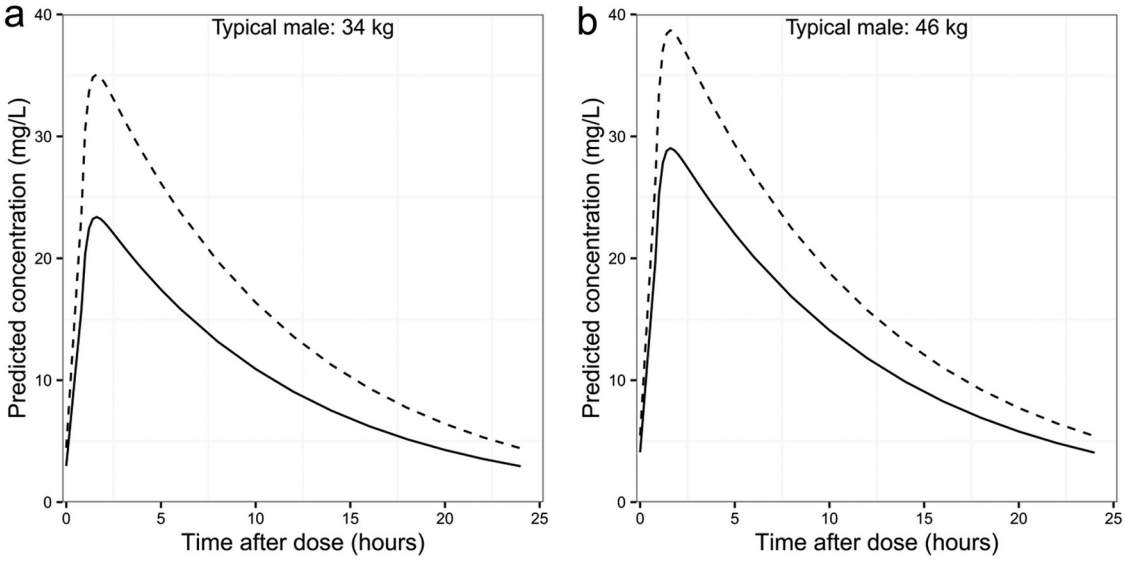


**FIG 3** (a) Predicted concentrations for a typical male patient weighing 34 kg, receiving 800 mg (solid line) and 1,200 mg (dashed line). (b) Predicted concentrations for a typical male patient weighing 46 kg, receiving 1,200 mg (solid line) and 1,600 mg (dashed line).

of weight on both CL/*F* and *V*/*F* and also reported higher *V*/*F* in males than females (16% more). More recently, Chigutsa et al. (20) proposed a model incorporating allometric scaling using total body weight and reported larger bioavailability in women. When we accounted for body size using total body weight instead of FFM, the model estimated bioavailability among females to be 26% higher, the same effect observed by Chigutsa et al. Both results discussed above are consistent with ours, although the covariate effects were accounted for differently. By using allometric scaling to explain variability in body size, we apply a well-known concept without estimating any additional parameters (23). We believe that this strategy, also applied by Denti et al. (24) and Rockwood et al. (25), of describing the differences as being due to differences in size and body composition is both more parsimonious and physiologically plausible. Fur-

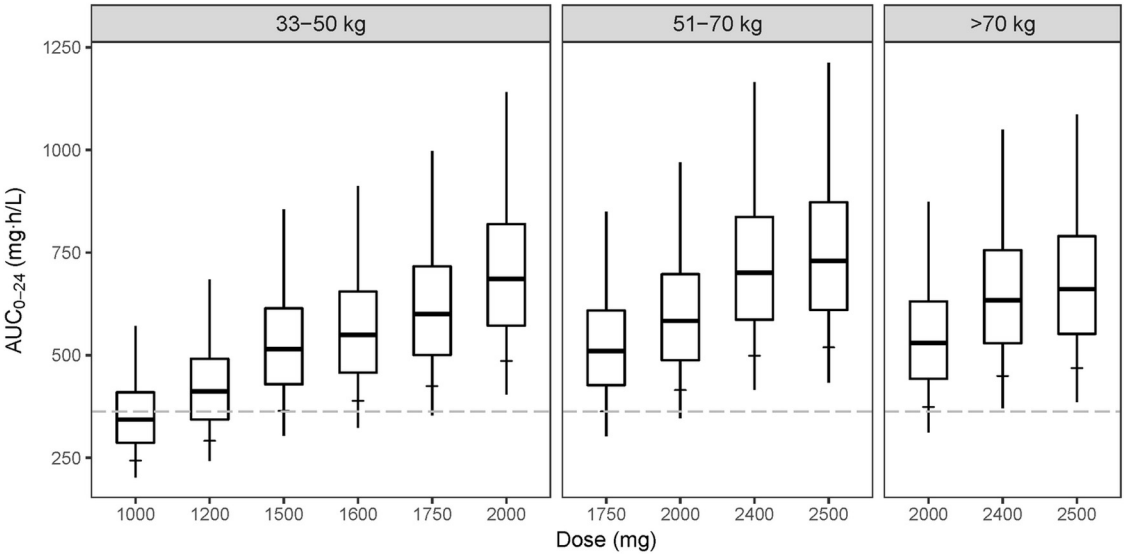


**FIG 4** Box plots of simulated $AUC_{0-24}$ achieved during treatment of MDR-TB using the model without the increase in clearance over time, stratified by weight band and dose administered. Single-dose tablets of pyrazinamide were used in the simulations, with each tablet containing either 400 mg, 500 mg, or 700 mg. The minimum and maximum values of the box plots are the 2.5th and 97.5th percentiles, and the horizontal tick mark on each box plot shows the 10th percentile. The dashed line represents the $AUC_{0-24}$ of 363 mg · h/liter.

thermore, this strategy has also been reported for other drugs in the FDC (24–28); hence, dosing regimens using current FDCs could be modified to take into account the variability in body size and composition.

Clearance of pyrazinamide was found to increase from the first day to day 29. The increase in clearance with time on treatment has been described by Smythe and Denti et al., with a later report of a 16% increase among Tanzanian patients, which is close to our 14% (24, 29). Symthe reported a higher increase (30%) in clearance from the first day to steady state in a cohort of TB patients from West Africa. The exact mechanism driving this change needs further investigation, and a number of reasons might explain this. Rifampin is a potent inducer of a large number of metabolic pathways via PXR (4). Induction of microsomal deamidase and xanthine oxidase enzymes responsible for pyrazinamide metabolism by rifampin might explain the observed result. Tuberculosis has been reported to lower drug-metabolizing capacity in animals (30), hence, treatment and improvement of the disease symptoms may enhance drug metabolism and other body functions, consistent with the observed increase in pyrazinamide clearance. Our estimated value of CL/*F* on day 29 is comparable to those reported in other studies, conducted in healthy volunteers, TB patients, and HIV/TB-coinfected patients (19, 21, 31). However, when predicting appropriate doses for patients with MDR-TB, we assumed a constant clearance over time, as the regimens used do not contain rifampin and the response to treatment is generally more gradual with the weaker second-line regimens than for patients with drug-susceptible TB.

Parameter estimates of the final model were used to simulate pyrazinamide exposure under different dosing schemes so as to achieve comparable $AUC_{0-24}$ values across weight bands. Consistent with the previous noncompartmental analysis (NCA) of the data (17), our model predicted that patients in lower weight bands attain lower drug exposures than those in the 55- to 70-kg weight band despite administering similar weight-adjusted doses. Disease severity is associated with low body mass index (32). Lower pyrazinamide exposure among these patients is likely to be even more critical and is associated with poor treatment outcomes (5, 11). Alternative doses for the treatment of drug-susceptible TB suggested in this report are based on the current weight bands and available FDC tablet sizes or single pyrazinamide tablets, each at a strength of 400 mg. Implementation of a fixed pyrazinamide dose of 1,500 mg as proposed by Sahota and Della Pasqua might be challenging under the current FDC therapy. Moreover, while desirable in terms of simplification, it implies reducing exposures of pyrazinamide and other drugs among patients with weight greater than 54 kg, thereby increasing the risks of poor treatment outcomes (18). The distribution of model-predicted $AUC_{0-24}$ suggests that adding 400 mg of pyrazinamide to the current FDC for patients with weights less than 55 kg (alternative dosing strategy 2) would achieve more uniform exposures across weight bands and increase the proportion of patients attaining an $AUC_{0-24}$ of 363 mg · h/liter. The same dosing strategy will result in the majority of patients attaining a $C_{max}$ of 35 mg/liter, which was found to be associated with favorable treatment outcomes (11). McIlleron et al. reported reduced exposure to drugs in FDC among patients who are male or with low weight (17), hence our proposed optimal dosing strategy could be transferable to other drugs of the FDC. Another advantage of the proposed dosing strategy is the reduction of weight bands from 4 to 3, where the 38- to 54-kg and 55- to 70-kg weight bands are combined. There would be a slight gain in the proportion of patients achieving the target $AUC_{0-24}$ overall under the alternative dosing strategy 3 compared to alternative 2, but the risk of hepatotoxicity could be elevated for patients in the 30- to 37-kg weight band treated under the alternative dosing strategy 3, who would be administered between 42 and 53 mg/kg doses (33).

The currently recommended pyrazinamide dose of 30 to 40 mg/kg results in disparate exposure among patients with MDR-TB (15). Moreover, a significant proportion of patients treated according to the recommended dose do not achieve the therapeutic $AUC_{0-24}$ of 363 mg · h/liter identified for drug-susceptible TB. Assuming availability of 400-, 500-, and 750-mg tablet sizes, our simulations predict that prescrip-

tion of doses at the higher end of the recommended range for low-weight patients will help minimize the differences in exposure between weight bands. Our proposed optimal dosing strategy of 1,500 mg for patients in the 33- to 50-kg weight band, 1,750 mg for patients weighing up to 70 kg, and 2,000 mg for heavier patients ensures that exposures between weight bands are comparable. Furthermore, the strategy guarantees that 90% of MDR-TB patients achieve exposures of >363 mg · h/liter.

The model presented here has some limitations. A simple linear change in clearance over time from initiation of treatment was assumed, hence limiting our capacity to extrapolate from our results beyond observed day 29. On the other hand, since the values of CL on day 29 are similar to those of prior reports, one can speculate that the change in clearance after the first month is not as large as the one observed in the first month of treatment. Our simulations were based on the assumption of first-order elimination. Since pyrazinamide is eliminated mainly as metabolites through multiple pathways (20, 34), if one or more of these pathways were to saturate at higher doses, the model may be underpredicting exposure in lower weight bands. The model developed was based on PK from a single study population. However, demographic characteristics broadly representing an African population were used in the simulations to account for a key covariate effect (FFM) during simulations, hence the use of FFM values outside the range that was used to optimize parameter estimates of the model. The demographic characteristics of patients with drug-susceptible TB were assumed to be similar to those of MDR-TB patients in the simulations, but there could be differences between the two groups of patients in terms of disease chronicity and severity that may influence pharmacokinetics and pharmacokinetic targets. Another limitation of the study is the nonavailability of MIC distribution for calculation of AUC/MIC ratio as a pharmacodynamic index. However, the range of MICs for drug-susceptible and MDR-TB are comparable as reported by Chigutsa et al. and Zheng et al., respectively (12, 35). Regardless of the therapeutic index used (AUC or AUC/MIC), the target will be affected by activity of concomitant drugs as well as the synergy or antagonism with pyrazinamide, demonstrated with rifampin and bedaquiline (12, 36).

In conclusion, our data in patients on the standard rifampin-based first-line regimen suggest that there is an increase in clearance of pyrazinamide during the first month of treatment. The currently recommended doses of pyrazinamide result in different levels of exposure among patients in the different weight bands. More uniform exposures with more patients attaining target exposures would be achieved by adding 400 mg to the dose for patients weighing between 30 and 54 kg. Reduced exposure to other drugs of the FDC has been reported among patients with low weight; hence, an alternative 2 dosing strategy could be applied to all four drugs by adding one FDC tablet. While it is necessary to confirm our findings in patients with MDR-TB, our analysis suggests that average pyrazinamide exposure in different weight bands could be made uniform by administering 1,500 mg to those with weights of at most 50 kg and 1,750 mg and 2,000 mg to those in the 51- to 70-kg and >70-kg weight bands, respectively.

## MATERIALS AND METHODS

This report is a model-based secondary analysis of a study described before. The original report includes a detailed description of the study design, including patient selection, inclusion and exclusion criteria, informed consent, adherence monitoring, and blood sample collection (17). Briefly, patients were administered 4-drug FDC tablets, each containing 150 mg of rifampin, 75 mg of isoniazid, 400 mg of pyrazinamide, and 275 mg of ethambutol. Individual doses were adjusted based on body weight according to WHO guidelines (14), with 51/61 patients receiving the medications daily from Monday to Friday and the remaining 10 every day of the week.

Pharmacokinetic blood sampling was performed on the 1st, 8th, 15th, and 29th day of TB treatment after an overnight fast. Samples were collected immediately before the dose and at 1, 2, 4, 6, 8, and 12 h postdose. An additional sample was collected at approximately 12 h before the dose administered on the 15th day. Details of procedure and methods used for separation of plasma, storage of samples, and quantification of drug concentrations were as described in a previous report (17). The lower limit of quantification for the assay was 0.2 mg/liter.

Pyrazinamide concentrations were described using nonlinear mixed-effects modeling using the software NONMEM 7.3 (37) and the first-order conditional estimation method with eta-epsilon interac-

tion (FOCE-I). Model diagnostics and documentation of model development were performed using Perl-speaks-NONMEM (PsN), Pirana, and Xpose (R package) (38). Additional plots were generated using R, version 3.2.1 (39), via RStudio, version 0.98.1091 (40).

**Model development.** One- and two-compartment disposition models with first-order elimination and different absorption models, including first-order absorption with and without lag time and a more flexible transit compartment absorption (41), were assessed. Plots of random effects of PK parameters were generated to identify trends in pharmacokinetic parameters with time on treatment. Three approaches to characterize the change in clearance over time were explored: estimating a separate value of clearance at each sampling day, an exponential increase in clearance from the first day to day 29 (exponential induction model), and linear increase in clearance from day 1 to day 29. The exponential induction model characterizing clearance on each day was parameterized using clearance on the first day ($CL_{day\ 1}$), change in clearance at day 29 ($\Delta CL_{day\ 29}$), and a half-life of the exponential process ($t_{50}$), as in equation 1. In the equation, the time variable for days on treatment went from 0 (day 1) to 28 (day 29).

$$CL_{day} = CL_{day1} + \Delta CL_{day29} \cdot CL_{day1} \cdot \left( \frac{1 - e^{\frac{-\ln(2)\cdot time}{t_{50}}}}{1 - e^{\frac{-\ln(2)\cdot 28}{t_{50}}}} \right) \quad (1)$$

The model with a linear increase in clearance was parameterized using clearance at baseline (day 1) and change in clearance on day 29 ($\Delta CL_{day\ 29}$), and the relationship is shown in equation 2. Similar to the exponential induction model, time on treatment was recorded from day 0 (day 1) to 28 (day 29).

$$CL_{day} = CL_{day1} + \Delta CL_{day29} \cdot CL_{day1} \cdot \frac{time}{28} \quad (2)$$

Allometric scaling was applied testing either total body weight (TBW) or fat-free mass (FFM) as a body size descriptor. The allometry exponents were either estimated or fixed to 0.75 for CL and 1 for *V*, as suggested by Anderson and Holford (23). Individual values of FFM ($FFM_i$) were calculated using the following formula:

$$FFM_i = \frac{WHS_{max} \cdot Height^2 \cdot Weight}{WHS_{50} \cdot Height^2 + Weight} \quad (3)$$

The maximal weight height squared ($WHS_{max}$) is 42.92 kg/m$^2$ for males and 37.99 kg/m$^2$ for females. The $WHS_{50}$ has values of 30.93 kg/m$^2$ for males and 35.98 kg/m$^2$ for females (42).

The typical value of bioavailability was fixed to a reference value of 1. Between-subject variability (BSV) and between-occasion variability (BOV) in the PK parameters were explored assuming log-normal distribution. An error model with both additive and proportional components was used to describe residual unexplained variability. Model building was guided by a change in objective function value (ΔOFV; assumed to be approximately $\chi^2$ distributed), inspection of diagnostic plots, including prediction-corrected visual predictive check (PcVPC) (43), and physiological plausibility. The effect of $CD4^+$ count, viral load, early antiretroviral therapy (ART) initiation, alanine transaminase (ALT), albumin, creatinine clearance, and formulation on PK parameters was assessed by exploring proportional changes in parameter estimates per unit of difference from the median for continuous covariates or relative changes from a reference category for categorical variables as described by Mould and Upton (44). Creatinine clearance was calculated from serum creatinine using the Cockroft-Gault equation (45). The precision of parameter estimates of the final model was evaluated using a nonparametric bootstrap method with replacement ($n = 200$).

The final PK model was then used to simulate steady-state pyrazinamide concentrations achieved during the treatment of drug-susceptible TB and MDR-TB after administration of feasible doses based of WHO-defined weight bands. Simulations (1,000 repetitions) were performed using demographic data of 870 tuberculosis patients obtained from PK studies conducted in South Africa and West Africa (17, 29, 46–49). For drug-susceptible TB, dosing strategies were assessed using the current weight bands and currently available FDC tablet sizes or additional 400-mg pyrazinamide tablets. For each dosing strategy, the proportion of patients achieving a target $AUC_{0-24}$ of 363 mg · h/liter in each weight band was determined (5). In the simulations for MDR-TB, we used estimated PK parameters for day 1 of treatment to explore exposure associated with currently recommended doses: patients with between 33 and 50 kg receive 1,000 to 1,500 mg, while patients with weight between 51 and 70 kg and those above 70 kg receive 1,750 mg and 2,000 to 2,500 mg, respectively (15). Using the same weight bands and available single-dose tablet sizes of 400 mg, 500 mg, and 750 mg, we explored exposure obtained under different dosing strategies and identified the dose at which comparable exposure is attained in the different weight bands. Additionally, the proportion of patients achieving an $AUC_{0-24}$ of 363 mg · h/liter was evaluated, since there is limited information on AUC/MIC pharmacodynamic index for MDR-TB. However, the MIC distributions for pyrazinamide do not seem highly variable between patients with drug-susceptible or MDR-TB. Zheng et al. reported MIC values ranging from 6.2 mg/liter to 400 mg/liter among MDR-TB patients, and among patients with drug-susceptible tuberculosis, Chigutsa et al. reported MIC values from 12.5 mg/liter to >100 mg/liter (12, 35). Furthermore, using the clinical breakpoints suggested by Zheng et al. of 18.75 mg/liter and 37.5 mg/liter, associated with 4-month culture conversion and treatment success, respectively (35), and an $AUC_{0-24}$ of 363 mg · h/liter, the calculated AUC/MIC values are close to 11.3, as reported by Chigutsa et al. (12).

## ACKNOWLEDGMENTS

The study was sponsored by the Special Programme for Research and Training in Tropical Diseases, World Health Organization and United States Agency for

International Development (USAID; umbrella grant no. AAG-G-00-99-00005). M.T.C. is supported by the European & Developing Countries Clinical Trials Partnership (PACTR201105000291300). M.T.C. and H.M. are funded in part by the National Research Foundation, South Africa.

The Division of Clinical Pharmacology at the University of Cape Town gratefully acknowledges Novartis Pharma for their support of the development of pharmacometric skills in Africa.

## REFERENCES

1. Konno K, Feldmann FM, McDermott W. 1967. Pyrazinamide susceptibility and amidase activity of tubercle bacilli. Am Rev Respir Dis 95:461–469.
2. Mitchison DA. 1985. The action of antituberculosis drugs in short-course chemotherapy. Tubercle 66:219–225. https://doi.org/10.1016/0041-3879(85)90040-6.
3. Steele MA, Des Prez RM. 1988. The role of pyrazinamide in tuberculosis chemotherapy. Chest 94:845–850. https://doi.org/10.1378/chest.94.4.845.
4. Chen J, Raymond K. 2006. Roles of rifampicin in drug-drug interactions: underlying molecular mechanisms involving the nuclear pregnane X receptor. Ann Clin Microbiol Antimicrob 5:3.
5. Pasipanodya JG, McIlleron H, Burger A, Wash PA, Smith P, Gumbo T. 2013. Serum drug concentrations predictive of pulmonary tuberculosis outcomes. J Infect Dis 208:1464–1473. https://doi.org/10.1093/infdis/jit352.
6. Mitchison DA, Fourie PB. 2010. The near future: improving the activity of rifamycins and pyrazinamide. Tuberculosis 90:177–181. https://doi.org/10.1016/j.tube.2010.03.005.
7. Diacon AH, Dawson R, von Groote-Bidlingmaier F, Symons G, Venter A, Donald PR, van Niekerk C, Everitt D, Winter H, Becker P, Mendel CM, Spigelman MK. 2012. 14-day bactericidal activity of PA-824, bedaquiline, pyrazinamide, and moxifloxacin combinations: a randomised trial. Lancet 380:986–993. https://doi.org/10.1016/S0140-6736(12)61080-0.
8. Zhang Y, Mitchison D. 2003. The curious characteristics of pyrazinamide: a review. Int J Tuberc Lung Dis 7:6–21.
9. Heifets L, Lindholm-Levy P. 1992. Pyrazinamide sterilizing activity in vitro against semidormant Mycobacterium tuberculosis bacterial populations. Am Rev Respir Dis 145:1223–1225. https://doi.org/10.1164/ajrccm/145.5.1223.
10. Mitchison DA. 2005. The diagnosis and therapy of tuberculosis during the past 100 years. Am J Respir Crit Care Med 171:699–706. https://doi.org/10.1164/rccm.200411-1603OE.
11. Chideya S, Winston CA, Peloquin CA, Bradford WZ, Hopewell PC, Wells CD, Reingold AL, Kenyon TA, Moeti TL, Tappero JW. 2009. Isoniazid, rifampin, ethambutol, and pyrazinamide pharmacokinetics and treatment outcomes among a predominantly HIV-infected cohort of adults with tuberculosis from Botswana. Clin Infect Dis 48:1685–1694. https://doi.org/10.1086/599040.
12. Chigutsa E, Pasipanodya JG, Visser ME, van Helden PD, Smith PJ, Sirgel FA, Gumbo T, McIlleron H. 2015. Impact of nonlinear interactions of pharmacokinetics and MICs on sputum bacillary kill rates as a marker of sterilizing effect in tuberculosis. Antimicrob Agents Chemother 59:38–45. https://doi.org/10.1128/AAC.03931-14.
13. Gumbo T, Chigutsa E, Pasipanodya J, Visser M, van Helden PD, Sirgel FA, McIlleron H. 2014. The pyrazinamide susceptibility breakpoint above which combination therapy fails. J Antimicrob Chemother 69:2420–2425. https://doi.org/10.1093/jac/dku136.
14. World Health Organization. 2003. Treatment of tuberculosis: guidelines for national programmes, 3rd ed. WHO/CDS/TB/2003.313. World Health Organization, Geneva, Switzerland.
15. World Health Organization. 2009. Management of MDR-TB: a field guide. A companion document to guidelines for the programmatic management of drug-resistant tuberculosis. WHO/HTM/TB/2008.402a. World Health Organization, Geneva, Switzerland.
16. Shih T-Y, Pai C-Y, Yang P, Chang W-L, Wang N-C, Hu OY-P. 2013. A novel mechanism underlies the hepatotoxicity of pyrazinamide. Antimicrob Agents Chemother 57:1685–1690. https://doi.org/10.1128/AAC.01866-12.
17. McIlleron H, Rustomjee R, Vahedi M, Mthiyane T, Denti P, Connolly C, Rida W, Pym A, Smith PJ, Onyebujoh PC. 2012. Reduced antituberculosis drug concentrations in HIV-infected patients who are men or have low weight: implications for international dosing guidelines. Antimicrob Agents Chemother 56:3232–3238. https://doi.org/10.1128/AAC.05526-11.
18. Sahota T, Della Pasqua O. 2012. Feasibility of a fixed-dose regimen of pyrazinamide and its impact on systemic drug exposure and liver safety in patients with tuberculosis. Antimicrob Agents Chemother 56:5442–5449. https://doi.org/10.1128/AAC.05988-11.
19. Wilkins JJ, Langdon G, McIlleron H, Pillai GC, Smith PJ, Simonsson US. 2006. Variability in the population pharmacokinetics of pyrazinamide in South African tuberculosis patients. Eur J Clin Pharmacol 62:727–735. https://doi.org/10.1007/s00228-006-0141-z.
20. Chigutsa E, Mcilleron H, Holford NHG. 2010. Parallel first order and mixed order elimination of pyrazinamide in South African patients with tuberculosis. Abstr Pop Approach Group Eur Meeting, abstr 1496.
21. Zhu M, Starke JR, Burman WJ, Steiner P, Stambaugh JJ, Ashkin D, Bulpitt AE, Berning SE, Peloquin CA. 2002. Population pharmacokinetic modeling of pyrazinamide in children and adults with tuberculosis. Pharmacotherapy 22:686–695.
22. Peloquin CA, Bulpitt AE, Jaresko GS, Jelliffe RW, James GT, Nix DE. 1998. Pharmacokinetics of pyrazinamide under fasting conditions, with food, and with antacids. Pharmacotherapy 18:1205–1211.
23. Anderson BJ, Holford NHG. 2008. Mechanism-based concepts of size and maturity in pharmacokinetics. Annu Rev Pharmacol Toxicol 59:303–332. https://doi.org/10.1146/annurev.pharmtox.48.113006.094708.
24. Denti P, Jeremiah K, Chigutsa E, Faurholt-Jepsen D, PrayGod G, Range N, Castel S, Wiesner L, Hagen CM, Christiansen M, Changalucha J, McIlleron H, Friis H, Andersen AB. 2015. Pharmacokinetics of isoniazid, pyrazinamide, and ethambutol in newly diagnosed pulmonary TB patients in Tanzania. PLoS One 10:e0141002. https://doi.org/10.1371/journal.pone.0141002.
25. Rockwood N, Meintjes G, Chirehwa M, Wiesner L, McIlleron H, Wilkinson RJ, Denti P. 2016. HIV-1 coinfection does not reduce exposure to rifampin, isoniazid, and pyrazinamide in South African tuberculosis outpatients. Antimicrob Agents Chemother 60:6050–6059. https://doi.org/10.1128/AAC.00480-16.
26. Chirehwa MT, Rustomjee R, Mthiyane T, Onyebujoh P, Smith P, McIlleron H, Denti P. 2015. Model-based evaluation of higher doses of rifampin using a semimechanistic model incorporating autoinduction and saturation of hepatic extraction. Antimicrob Agents Chemother 60:487–494. https://doi.org/10.1128/AAC.01830-15.
27. Smythe W, Khandelwal A, Merle C, Rustomjee R, Gninafon M, Bocar Lo M, Sow OB, Olliaro PL, Lienhardt C, Horton J, Smith P, McIlleron H, Simonsson USH. 2012. A semimechanistic pharmacokinetic-enzyme turnover model for rifampin autoinduction in adult tuberculosis patients. Antimicrob Agents Chemother 56:2091–2098. https://doi.org/10.1128/AAC.05792-11.
28. Geiseler PJ, Manis RD, Maddux MS. 1985. Dosage of antituberculous drugs in obese patients. Am Rev Respir Dis 131:944–946.
29. Smythe WA. 2016. Characterizing population pharmacokinetic/pharmacodynamic relationships in pulmonary tuberculosis infected adults using nonlinear mixed effects modelling. Ph.D. thesis, University of Cape Town, Cape Town, South Africa. https://open.uct.ac.za/bitstream/item/23227/thesis_hsf_2016_smythe_wynand_anton.pdf.
30. Batra JK, Venkitasubramanian TA, Raj HG. 1987. Drug metabolism in experimental tuberculosis. I. Changes in hepatic and pulmonary monooxygenase activities due to infection. Eur J Drug Metab Pharmacokinet 12:109–114.
31. Peloquin CA, Jaresko GS, Yong CL, Keung AC, Bulpitt AE, Jelliffe RW. 1997. Population pharmacokinetic modeling of isoniazid, rifampin, and pyrazinamide. Antimicrob Agents Chemother 41:2670–2679.
32. Van Lettow M, Kumwenda JJ, Harries AD, Whalen CC, Taha TE, Kumwenda N, Kang'ombe C, Semba RD. 2004. Malnutrition and the severity

of lung disease in adults with pulmonary tuberculosis in Malawi. Int J Tuberc Lung Dis 8:211–217.
33. US Public Health Service. 1969. Hepatic toxicity of pyrazinamide used with isoniazid in tuberculous patients. Am Rev Respir Dis 59:13.
34. Lacroix C, Hoang TP, Nouveau J, Guyonnaud C, Laine G, Duwoos H, Lafont O. 1989. Pharmacokinetics of pyrazinamide and its metabolites in healthy subjects. Eur J Clin Pharmacol 36:395–400. https://doi.org/10.1007/BF00558302.
35. Zheng X, Zheng R, Hu Y, Werngren J, Forsman LD, Mansjö M, Xu B, Hoffner S. 2016. Determination of MIC breakpoints for second-line drugs associated with clinical outcomes in multidrug-resistant tuberculosis treatment in China. Antimicrob Agents Chemother 60:4786–4792. https://doi.org/10.1128/AAC.03008-15.
36. Field SK. 2015. Bedaquiline for the treatment of multidrug-resistant tuberculosis: great promise or disappointment? Ther Adv Chronic Dis 6:170–184. https://doi.org/10.1177/2040622315582325.
37. Beal S, Sheiner L, Boeckmann A, Bauer R. 2009. NONMEM users guides (1989-2009). ICON Development Solutions, Ellicott City, MD.
38. Keizer RJ, Karlsson MO, Hooker A. 2013. Modeling and simulation workbench for NONMEM: tutorial on Pirana, PsN, and Xpose. CPT Pharmacometrics Syst Pharmacol 2:e50. https://doi.org/10.1038/psp.2013.24.
39. Core Team R. 2014. R: a language and environment for statistical computing. Version 3.1.2. R Foundation for Statistical Computing, Vienna, Austria.
40. RStudio. 2014. RStudio: integrated development environment for R. Version 0.99.903. RStudio, Boston, MA.
41. Savic R, Jonker D, Kerbusch T, Karlsson M. 2007. Implementation of a transit compartment model for describing drug absorption in pharmacokinetic studies. J Pharmacokinet Pharmacodyn 34:711–726. https://doi.org/10.1007/s10928-007-9066-0.
42. Janmahasatian S, Duffull SB, Ash S, Ward LC, Byrne NM, Green B. 2005. Quantification of lean bodyweight. Clin Pharmacokinet 44:1051–1065. https://doi.org/10.2165/00003088-200544100-00004.
43. Bergstrand M, Hooker AC, Wallin JE, Karlsson MO. 2011. Prediction-corrected visual predictive checks for diagnosing nonlinear mixed-effects models. AAPS J 13:143–151. https://doi.org/10.1208/s12248-011-9255-z.
44. Mould DR, Upton RN. 2013. Basic concepts in population modeling, simulation, and model-based drug development-part 2: introduction to pharmacokinetic modeling methods. CPT Pharmacometrics Syst Pharmacol 2:e38. https://doi.org/10.1038/psp.2013.14.
45. Cockcroft DW, Gault MH. 1976. Prediction of creatinine clearance from serum creatinine. Nephron 16:31–41. https://doi.org/10.1159/000180580.
46. Chigutsa E, Visser ME, Swart EC, Denti P, Pushpakom S, Egan D, Holford NHG, Smith PJ, Maartens G, Owen A, McIlleron H. 2011. The SLCO1B1 rs4149032 polymorphism is highly prevalent in South Africans and is associated with reduced rifampin concentrations: dosing implications. Antimicrob Agents Chemother 55:4122–4127. https://doi.org/10.1128/AAC.01833-10.
47. Diacon AH, Patientia RF, Venter A, van Helden PD, Smith PJ, McIlleron H, Maritz JS, Donald PR. 2007. Early bactericidal activity of high-dose rifampin in patients with pulmonary tuberculosis evidenced by positive sputum smears. Antimicrob Agents Chemother 51:2994–2996. https://doi.org/10.1128/AAC.01474-06.
48. Pepper DJ, Marais S, Wilkinson RJ, Bhaijee F, Maartens G, McIlleron H, De Azevedo V, Cox H, McDermid C, Sokhela S, Patel J, Meintjes G. 2010. Clinical deterioration during antituberculosis treatment in Africa: incidence, causes and risk factors. BMC Infect Dis 10:83. https://doi.org/10.1186/1471-2334-10-83.
49. Wilkins JJ, Savic RM, Karlsson MO, Langdon G, McIlleron H, Pillai G, Smith PJ, Simonsson USH. 2008. Population pharmacokinetics of rifampin in pulmonary tuberculosis patients, including a semimechanistic model to describe variable absorption. Antimicrob Agents Chemother 52:2138–2148. https://doi.org/10.1128/AAC.00461-07.